DEUTSCHES ELEKTRONEN-SYNCHROTRON DESY

DESY SR-72/14
August 1972

Optical Absorption of Tellurium in the Region Between 39 and 250 eV

by

B. Sonntag, T. Tuomi, and G. Zimmerer
Deutsches Elektronen-Synchrotron DESY, Hamburg
and
II. Institut für Experimentalphysik der Universität Hamburg

2 HAMBURG 52 · NOTKESTIEG 1

To be sure that your preprints are promptly included in the HIGH ENERGY PHYSICS INDEX, send them to the following address (if possible by air mail):

DESY
Bibliothek
2 Hamburg 52
Notkestieg 1
Germany

Optical Absorption of Tellurium in the Region between 39 and 250 eV

B. Sonntag, T. Tuomi[+], and G. Zimmerer

Deutsches Elektronen-Synchrotron DESY, Hamburg, Germany

and

II. Institut für Experimentalphysik der Universität Hamburg,

Hamburg, Germany

The absorption spectrum of evaporated thin films of crystalline and amorphous tellurium was measured in the region between 39 and 250 eV. The electron synchrotron DESY was used as a light source. A sharp doublet around 42 eV and a weak structure on its high energy side associated with transitions from the spin-orbit split 4d core levels to the conduction band were observed and compared with the density of conduction states of crystalline tellurium and with the calculated multiplet splitting of the $4d^9 5p^5$ configuration of atomic Te. The doublet was also observed in the amorphous phase. At higher energies the absorption spectrum is dominated by a broad, large maximum at 87 eV. After a minimum at 165 eV the absorption increases again with increasing photon energy. This behavior is very similar to the absorption spectrum of solid and gaseous Xenon and is consequently explained by atomic d→f transitions.

[+] supported by the Alexander von Humboldt Foundation,

present address: Helsinki University of Technology, Otaniemi

Submitted to: Physica status solidi

I. INTRODUCTION

The optical properties of Te within the fundamental absorption region have been investigated in the past, e.g., by measuring the reflectance of single crystals [1-4], polycrystalline [5], and amorphous layers [6]. In some cases, by using normal Kramers-Kronig techniques, the spectral dependence of the real and imaginary part of the dielectric constant, ε_1 and ε_2 was evaluated from the reflection data. In the case of crystalline Te the ε_2-spectra are in fairly good agreement with a calculation of ε_2 [7] in the energy range from 0.3 to 11 eV including anisotropy of the spectrum when measuring with light polarized parallel or perpendicular to the trigonal axis of Te single crystals.

The observed structures of the optical spectra in the fundamental absorption region are due to electronic transitions from the valence bands of the $5s^2$ and $5p^4$ electrons to the conduction bands. The assignment of the optical structures, however, is complicated by the fact that for Te most of the corresponding electronic transitions are not well localized in $\vec{k}$-space [7]. Because both the valence and conduction bands are involved in those transitions the optical spectra cannot give detailed information on the separate bands.

One of the purposes of this work is to overcome these difficulties by measuring the 4d absorption of Te. From earlier investigations [8-11] the transitions from the 4d core levels to the conduction band are expected to occur at about 42 eV. Since the width of the 4d core levels is small in comparison to the width of the conduction band, the absorption spectrum should represent the density of states of the conduction band provided the one-electron approximation is still valid and the corresponding transition probabilities are not dependent on energy.

II. EXPERIMENT

A. Experimental Procedure

The electron synchrotron DESY was used as a light source for the absorption measurements, the experimental arrangement being described to some extent elsewhere [12,13]. Thin layers of Te were placed in the almost parallel beam of the continuous synchrotron radiation. The light transmitted through the samples was focused into the entrance slit of a 1 m Rowland grazing incidence monochromator by a concave mirror. A gold coated grating with 2,400 lines per mm and a blaze angle of $4^{\circ}16'$ was used in first order with an angle of incidence of $77^{\circ}14'$. The wavelength resolution of the instrument was 0.1 Å over the entire range of energy. An open magnetic multiplier (Bendix M 306) was mounted behind the exit slit moving along the Rowland circle. Current fluctuations in the accelerator were compensated for. Background noise was reduced by modulating the incoming light and using phase sensitive amplifiers. Thus all structures causing > 3 % change in the absorption coefficient were observed. A grazing incidence vacuum ultraviolet monochromator with fixed exit slit [14] was used for some of the measurements above 130 eV. To obtain the transmission of a sample the spectrum of an empty substrate was measured in the same way as that of the sample on the substrate.

The layers were prepared by vacuum evaporation at a pressure of about 10^{-6} Torr. The substrate were aluminum (20 to 40 $\mu g/cm^2$) and carbon (20 $\mu g/cm^2$) films supported by a 70 μm copper mesh; they were kept at room temperature during evaporation. Some of the samples were heated in a vacuum of 10^{-6} Torr up to 370 K for half an hour to ensure their crystallinity. Amorphous layers were prepared by vacuum deposition in situ

on a cold substrate (80 K). We know from electrical and optical measurements [15] that Te films prepared in this way are amorphous. The thickness of the samples ranged from 200 to 3000 Å and was measured during evaporation with a quartz film thickness monitor. After evaporation the thickness was again determined using the Tolansky method. The thickness of the disordered layers was not measured.

The measurements were performed at 300 K and 80 K. Al and Si films (thickness ~1000 Å) have been used as filters to suppress higher spectral orders reflected from the grating.

B. Results

1. Crystalline Te

The absorption spectrum of crystalline Te at 300 K is shown in Fig. 1. The errors of the absorption coefficient, α, which are mostly due to uncertainties in the sample thickness, are indicated by error bars.

At the low energy side, at 40.95 and 42.30 eV, a rather sharp doublet is observed together with some weak structures up to 50 eV. At higher energy the absorption coefficient increases strongly and reaches a broad prominent maximum at 87 eV. Two weak shoulders show up at 63 eV and 80 eV. The maximum is followed by a minimum at about 165 eV where α is as small as 3×10^4 cm^{-1}. Above this minimum α begins to increase slowly with increasing photon energy. The over-all spectral dependence and the absolute value of the absorption coefficient given by Lukirskii et al. [11] are in agreement with our results, whereas the absorption coefficient reported by Woodruff and Givens [8] is much larger.

The low energy doublet is shown in a larger scale in Fig. 2. The two peaks, D_1 and $D_1+\Delta d$, are due to transitions from the spin-orbit split 4d levels of Te to the conduction band. The energy separation Δd of these maxima of 1.35 eV is in rather good agreement with the values given by other authors [8-11] and also with the 1.47 eV calculated for the spin-orbit splitting of the 4d level [16]. Above 45 eV three weak structures D_2, $D_2+\Delta d$ and D_3 can be seen.

The part of the spectrum under consideration was also measured at liquid nitrogen temperature. No noticeable difference between the curves at both 300 K and 80 K was found either in the peak positions (shifts must be smaller than 0.05 eV) or in the overall shape. Additional structures could not be detected.

2. Amorphous Te

There is a considerable difference in the optical constants of crystalline and amorphous Te in the fundamental absorption region [6]; it is, therefore, expected that differences also occur in the VUV absorption spectrum, thus giving additional information on the electronic structure of disordered Te.

Figure 3 shows the absorption spectrum of amorphous Te. The doublet at 40.95 and 42.30 eV is as sharp in amorphous Te as in crystalline Te, and there is no shift in the positions of the peaks when going from the ordered to the disordered form. The only difference appears at photon energies larger than 47 eV. The peaks $D_2+\Delta d$, and D_3 in the crystalline material are smeared out in the amorphous state. Similar results were reported on Se where no difference has been found between the 3d absorption spectra of

the amorphous and the crystalline modification (17). The absolute value of the absorption coefficient at the low and high energy side of the doublet seems to be influenced by disorder. We cannot, however, exclude condensation on the surface of the layers kept at low temperature since the measurements were not performed in ultra high vacuum. Similar effects have been observed with crystalline samples cooled to 80 K.

III. THEORY AND DISCUSSION

For the purpose of discussion the measured absorption spectrum is divided into two parts. In the energy range from 39 eV to 52 eV the experimental results are compared to the calculated density of states of the conduction bands and to the calculated multiplet splitting of the $4d^9 5p^5$ configuration of atomic Te. In the other part of the spectrum, up to 250 eV, atomic effects are believed to dominate. This part of the spectrum is very similar to that of gaseous or solid iodine (18) and xenon (19) which are the next elements to Te in the periodic table.

A. Region from 39 eV to 52 eV

The density of states of the p_3- and the onset of the d-conduction band calculated by Maschke (20) is shown in Fig. 4. The p_3-density of states exhibits two main peaks which are well separated in energy by about 0.5 eV. Its width is 2 eV. The upper d-conduction band is clearly separated in energy from the p_3-conduction band by about 3.5 eV. This energy, however, is too large by about 1.5 eV. This may be concluded by comparing the results of the ε_2 calculation (7) with recent optical measurements (4), or more directly, by comparing the calculated density of states with photoemission results (20,21).

Starting with the result from Fig. 4, the calculated spectrum in Fig. 2 has been constructed in the following way. The density of states of Fig. 4 has been multiplied by 2/3 which corresponds to the statistical weight ratio of the $4d_{3/2}$ level to the $4d_{5/2}$ level. This spectrum has been shifted by the spin orbit energy of 1.35 eV upwards in the energy scale and added to the original density of states spectrum. In so doing it has been assumed that the transitions between the core levels and the conduction band can be described by constant transition probabilities. When comparing the calculated spectrum with the experimental one it is noticed that the total width of the measured doublet with a reasonable background substraction is in good agreement with the width of the calculated spectrum. The theoretical curve, however, clearly has four major peaks whereas in the experimental spectrum there are only two, although the experimental resolution was high enough to have detected those structures had they been there. The maximum $D_1+\Delta d$ round experimentally is strongly asymmetric with a tail on the high energy side extending up to about 3 eV above the maximum. Taking the same asymmetric shape for the first peak D_1 we find that the second peak $D_1+\Delta d$ is sitting on a strong high energy tail of D_1. This is in agreement with the expected intensity ratio of 3:2 of both components. According to the results of the band calculations there is almost no overlap between both components; peak $D_1+\Delta d$ should, therefore, be smaller than D_1. The upper d-conduction band has to be shifted by about 1.5 eV towards lower energies as has been discussed above. The onset of transitions to this band should, therefore, occur at about 44 eV. From the experimental curve it is impossible to exactly determine the onset of these transitions since one would have to separate their contribution to the absorption from the underlying high energy tail of D_1 and $D_1+\Delta d$ and the background due to valence band transitions. The states of the upper conduction band are, moreover, mainly d-symmetric.

Transitions from the 4d-levels to these states are optically forbidden. Consequently the transitions to the upper conduction band only give rise to weak absorption maxima D_2, $D_2+\Delta d$ and D_3.

Comparison between the experimental results and the calculated density of states leads to the conclusion that the structures found experimentally cannot be explained by the one-electron joint density of states alone. We don't believe that the inclusion of calculated one-electron matrix elements will really improve the situation. This has been shown, for example, in the case of the 2p absorption of solid Si [22]. The main reason for the discrepancy between the experimental results and the one-electron density of states is the localized character of inner shell excitations. This has been clearly demonstrated in the case of simple metals, transition metals (see e.g. Ref. 23 and references therein) and rare earths [24-27]. The localized character also influenced the inner shell spectra of semi-conductors and insulators. Prominent exciton lines have been found in the spectra of alkali-halides and solid rare gases (see e.g. Ref. 28 and references therein). The localized character of the excitations giving rise to these absorption lines is supported by the results of photoemission measurements [29,30].

The Te 4d hole is fairly localized and not much influenced by the surrounding atoms. At the onset of the Te 4d absorption transitions to the lowest empty p-symmetric states, originating from the bound 5p states of the free Te atom, take place. It is reasonable to assume that the electrons are not excited into band states uniformly distributed throughout the crystal but into states considerably localized around the atom on which the 4d hole is located. In this case the electron-hole interaction has to be taken into account.

Using a multi-configuration Hartree-Fock program developed by Froese Fischer [31] we calculated the multiplet splitting of the $4d^9 5p^5$ configuration of atomic Te. These calculations show that the Coulomb-interaction (F^0 (4d,5p) $\approx$ 12 eV, F^2 (4d,5p) $\approx$ 2.9 eV) and the exchange interaction (G^1 (4d,5p) $\approx$ 0.8 eV, G^3 (4d,5p) $\approx$ 0.7 eV) between electron and hole give rise to a series of multiplet split lines extending over an energy range of about 3 eV. This means that these lines are spread over an energy range comparable to the width of the low energy doublet $D_1, D_1+\Delta d$. The multiplet splitting is, moreover, of the same order of magnitude as the width of the p-symmetric lower conduction bands. The electron-hole interaction will be overestimated by this simple atomic model but it will certainly not be negligible in solid Te. Lifetime broadening due to the decay of the localized states into continuum band states possibly smears out any sharp structure.

Calculations for the Se $3d^9 4p^5$ configuration give similar results. The reason for better agreement between the experimentally determined Se 3d absorption spectrum and the one-electron density of states is still unknown [17].

With the exception of the sharp excitonic lines Rössler [32] found reasonable agreement between the calculated density of states and the absorption spectrum at the onset of Xe 4d transitions. This indicates that the electron-hole interaction is smaller in the case of the Xe 4d absorption than in the case of the Te 4d absorption. Calculations for the $4d^9$ 6p configuration of atomic Xe support this suggestion. Due to the filled 5p shell the electron-hole interaction is drastically reduced.

Taking into account the localized character of the excitations at the onset of the Te 4d-absorption the result obtained for amorphous Te is not sur-

prising. Moreover, most recent density of states calculations for amorphous Te by Kramer [33], which are based on the CBS-method [33], show that the two main peaks of the p_3-conduction band even exist in disordered Te, whereas the d-conduction band is broadened and no longer has any structure. This explains the smearing out of the experimental curve above the prominent doublet.

B. Region from 52 eV to 250 eV

The over-all shape of the absorption spectrum of Te at photon energies larger than 52 eV can be understood, as has already been pointed out by Lukirskii et al. [11], at least qualitatively, in terms of a one-electron model for free atoms. For comparative purposes the results of McGuire's calculations [34] are shown together with the absorption spectrum in Fig. 1.

The broad maximum experimentally found at 87 eV is due to d→f transitions. These transitions are depressed at threshold and shifted to higher energies by a potential barrier [35]. It has been shown both theoretically [35] and experimentally [19,36] that these delayed transitions give rise to a particularly strong maximum when there are unoccupied f-states belonging to the same shell as the initially filled d-levels.

There are striking differences between theory and experiment. The theory yields a resonance maximum which is much stronger and sharper and occurs at an energy lower than experimentally observed. This is a general feature of one-electron calculations. Better agreement has been achieved by taking configuration interaction and electron correlation into account [24,27,37].

The shoulders at 63 eV and 80 eV may be due to the simultaneous excitation of a 4d electron and a valence electron. Similar double excitations have been detected in the 4d absorption spectra of gaseous I_2 [18] and Xe [38], and in the spectra of solid Xe [19] and solid Cs-halides [36].

According to McGuire's results the transition probability of the d→f transitions reaches a minimum at about 160 eV. The total absorption coefficient calculated by adding the contribution of the 4d, 4p, and 4s subshells does not show such a marked minimum as found experimentally.

Transitions with an initial state at the 4p core level and a final state in the conduction band are not observed around 110 eV. There are several reasons for this behavior of the absorption spectrum. Because of the atomic selection rules transitions to the first conduction band p_3, which is mainly p symmetric, are very improbable. McGuire's calculations [34] for free Te atoms show that the oscillator strengths of 4p→s and 4p→d transitions are small at threshold. Furthermore, lifetime broadening of the 4p levels smears out any structure. The same reasons hold for the transitions from the 4s levels. There is no structure at 168 eV where the onset of these transitions should occur [39].

To get a more quantitative understanding of the spectrum we have calculated N_{eff}, the effective number of electrons whose oscillator strength is exhausted within the energy range covered by our measurements,

$$N_{eff} = \frac{mcA}{\pi e^2 L \rho} \int_{E_1}^{E_2} \alpha n dE$$

with Avogadro's number L, atomic weight A, and density ρ. The real part of the refractive index n can be set equal to 1 in the energy region under

discussion. The number of 12.4 effective electrons contributing to absorption between 36 eV and 250 eV lies well below the number of 18 which one obtains by adding the 10 4d, the 6 4p, and the 2 4s electrons together. This leads to the conclusion that the oscillator strengths of transitions from these levels are not exhausted at 250 eV, thus being in agreement with McGuire's results. The contribution of valence band transitions should be small in this energy region.

ACKNOWLEDGMENTS

The authors would like to thank Dr. K. Maschke for stimulating discussions and for making available the results of his density of states calculations prior to publication. We appreciate the help of H.W. Wolff in handling the computer programs. Thanks are due to the Deutsche Forschungsgemeinschaft for financial support.

Literature

1. J. Stuke and H. Keller, phys.stat.sol. 7, 189 (1964)
2. H. Merdy, Ann.Phys. (Paris) 14e Sér. 1, 289 (1966)
3. S. Tutihasi, G.G. Roberts, R.C. Keezer, and R.E. Drews, Phys.Rev. 177, 1143 (1969)
4. P. Bammes, R. Klucker, E.E. Koch, and T. Tuomi, phys.stat.sol. (b) 49, 561 (1972)
5. J.D. Hayes, Jr., E.T. Arakawa, and M.W. Williams, J.Appl.Phys. 39, 5527 (1968)
6. J. Stuke and G. Zimmerer, to be published
7. K. Maschke, phys.stat.sol. (b) 47, 511 (1971)
8. R.W. Woodruff and M.P. Givens, Phys.Rev. 97, 52 (1955)
9. M.P. Givens, C.J. Koester, and W.L. Goffe, Phys.Rev. 100, 1112 (1955)
10. S. Robin-Kandare, J. des Recherches des C.N.R.S. No. 49, 311 (1959)
11. A.P. Lukirskii, T.M. Zimkina, and S.A. Gribovskii, Soviet Physics Solid State 8, 1525 (1966)
12. R.P. Godwin, in Springer Tracts in Modern Physics, ed. G. Höhler (Springer Verlag, Berlin 1969), vol. 51
13. P. Rabe, B. Sonntag, T. Sagawa, and R. Haensel, phys.stat.sol. (b) 50, 559 (1972)
14. H. Dietrich and C. Kunz, Rev.Sci.Instr. 43, 434 (1972)
15. H. Keller and J. Stuke, phys.stat.sol. 8, 831 (1965)
16. G.G. Wepfer, T.C. Collins, and R.N. Euwema, Phys.Rev. B4, 1296 (1971)
17. M. Cardona, W. Gudat, B. Sonntag, and P.Y. Yu, Proceedings Tenth International Conference on the Physics of Semiconductors, Aug. 1970, Cambridge, Mass.
18. F.J. Comes, U. Nielsen, and W.H.E. Schwarz, to be published
19. R. Haensel, G. Keitel, P. Schreiber, and C. Kunz, Phys.Rev. 188, 1375 (1969)

20. L.D. Laude, B. Fitton, B. Kramer, K. Maschke, to be published

21. L.D. Laude, B. Fitton, M. Anderegg, Phys.Rev. Letters 26, 637 (1971)

22. J.P. Van Dyke, Phys.Rev. B5, 4206 (1972)

23. see e.g. C. Kunz
Proc. Colloque C.N.R.S. "Processus électroniques simples et multiples du domaine X et X-UV", Paris, Sept. 1970
J. de Physique Tome 32 - C4, p. 180 and references therein

24. J.L. Dehmer, A.F. Starace, U. Fano, J. Sugar, and J.W. Cooper, Phys.Rev. Letters 26, 1521 (1971)

25. A.F. Starace, Phys.Rev. B5, 1773 (1972)

26. J. Sugar, Phys.Rev. B5, 1785 (1972)

27. J.L. Dehmer, A.F. Starace, Phys.Rev. B5, 1792 (1972)

28. see e.g. R. Haensel and B. Sonntag
Computational Solid State Physics, Proceedings of an International Symp. October 6-8, 1971, Wildbad Germany ed. F. Herman, N.W. Dalton, Th.R. Koehler (Plenum Press New York - London 1972) and references therein

29. D. Blechschmidt, M. Skibowski, and W. Steinmann, phys.stat.sol. 42, 61 (1970)

30. R. Haensel, G. Keitel, G. Peters, P. Schreiber, B. Sonntag, and C. Kunz, Phys.Rev. Letters 23, 530 (1969)

31. Ch. Froese Fischer, Computer Physics Communications 1, 151 (1969)

32. U. Rössler, phys.stat.sol. (b) 45, 483 (1971)

33. B. Kramer, phys.stat.sol. 41, 649 (1970)
B. Kramer, phys.stat.sol. 41, 725 (1970)

34. E.J. McGuire, Research Report SC-RR-721 Sandia Laboratories (1970)

35. U. Fano and J.W. Cooper, Rev.Mod.Phys. 40, 441 (1968)

36. M. Cardona, R. Haensel, D.W. Lynch, and B. Sonntag, Phys.Rev. B2, 1117 (1970)

37. M. Ya. Amusia, N.A. Cherepkov, and L.V. Chernysheva, Soviet Physics JETP 33, 90 (1971)

38. K. Codling and R.P. Madden, Appl.Opt. 4, 1431 (1965)

39. J.A. Bearden and A.F. Burr, Rev.Mod.Phys. 39, 125 (1967)

Figure captions

Fig. 1 Absorption coefficient of crystalline Te as a function of photon energy (solid line). Included are the results of McGuire's calculations (34) for atomic Te (dashed line). The values for the energy levels are taken from Ref. 39.

Fig. 2 Absorption spectrum of crystalline Te at room temperature near the onset of 4d-electron excitation and the spectrum calculated on the basis of the density of conduction states. The energy position of the theoretical curve has been adjusted to the experimental results.

Fig. 3 Absorption spectrum of amorphous Te at the onset of 4d transitions measured at 80 K.

Fig. 4 Density of conduction states of crystalline Te.

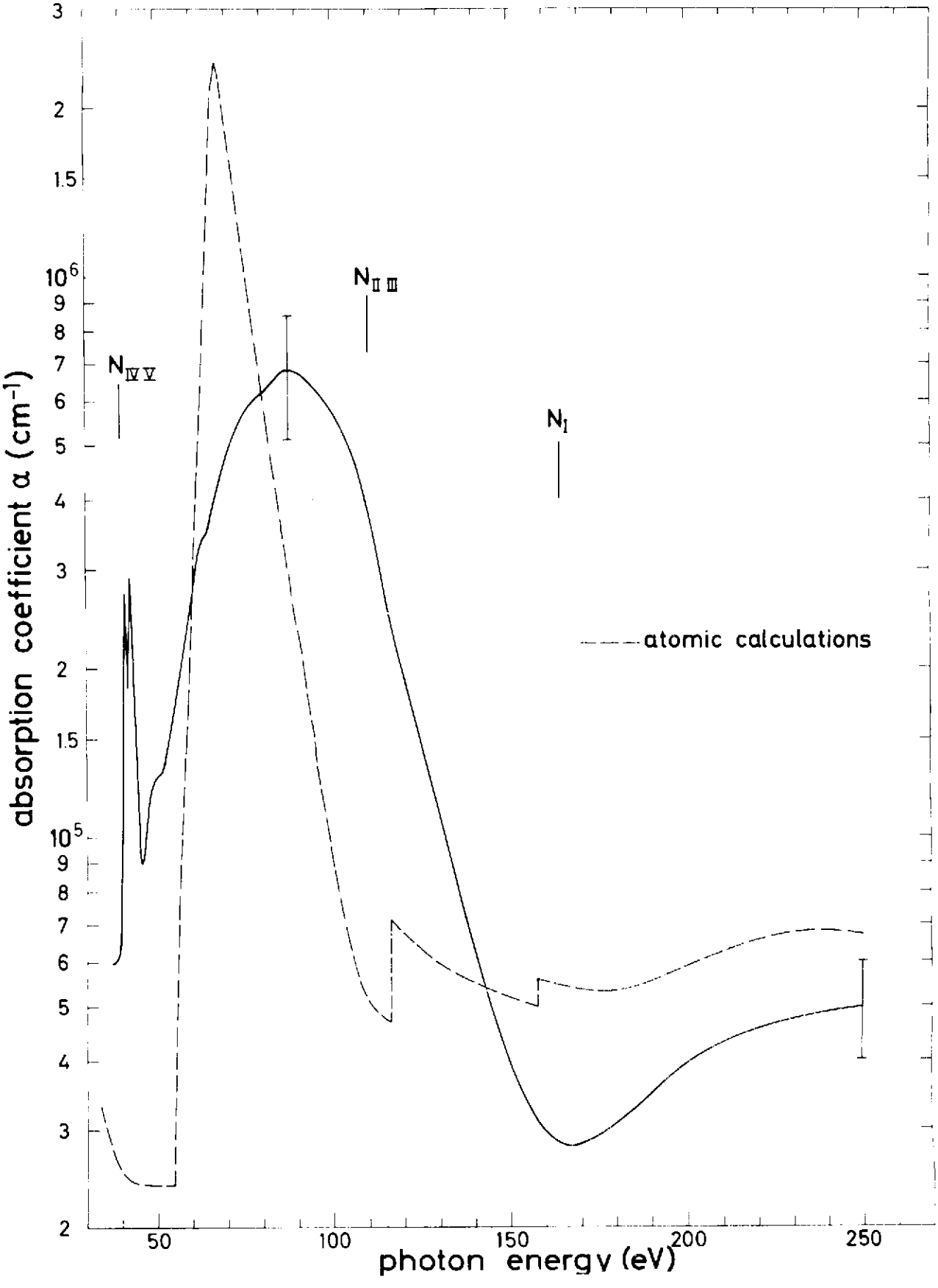
absorption coefficient α (cm⁻¹)
photon energy (eV)
N IV V
N II III
N I
atomic calculations
3
2
1.5
10⁶
9
8
7
6
5
4
3
2
1.5
10⁵
9
8
7
6
5
4
3
2
50
100
150
200
250

FIG.1

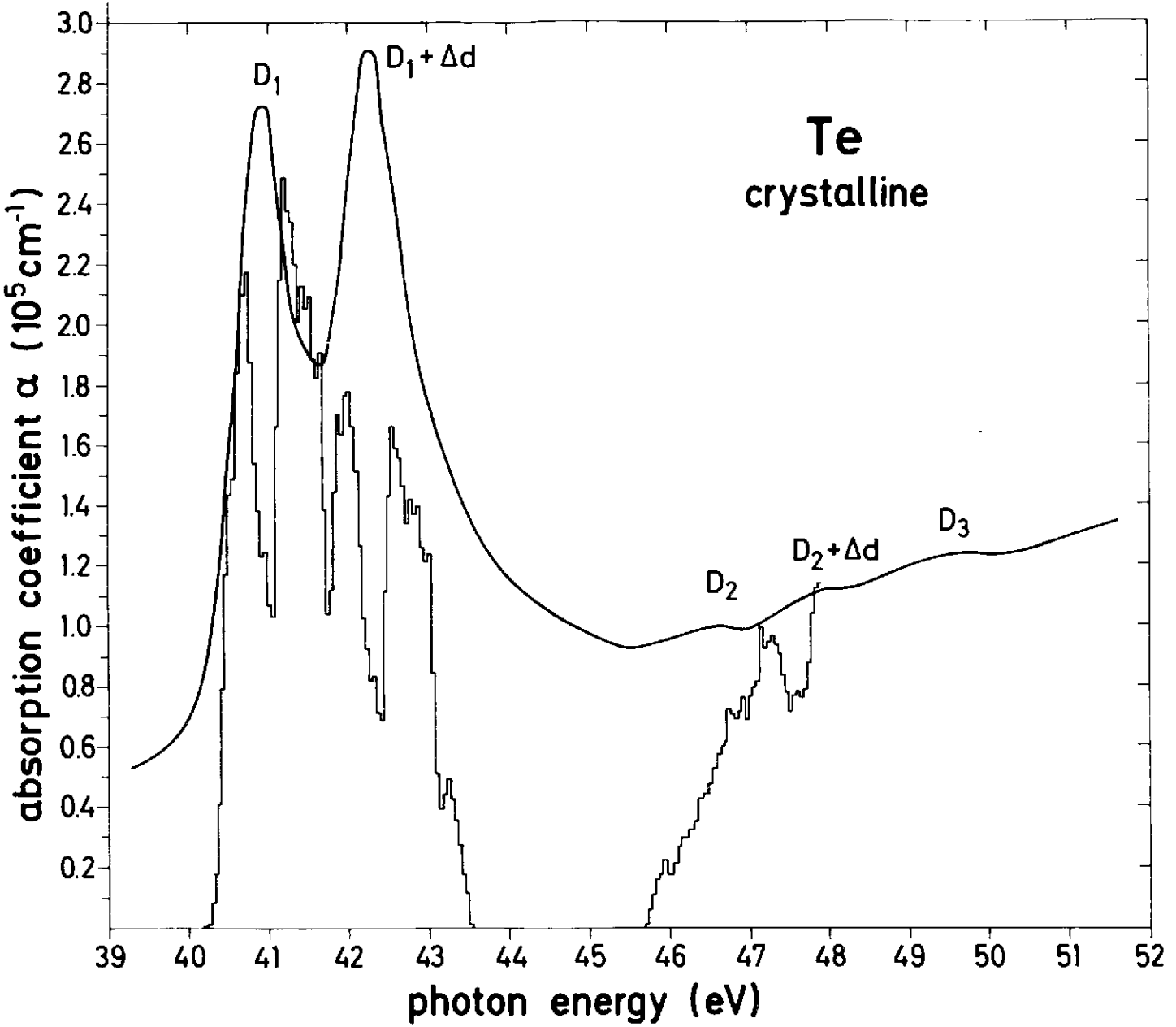
Te
crystalline
D1
D1 + Δd
D2
D2 + Δd
D3
absorption coefficient α (10^5 cm^-1)
photon energy (eV)
3.0
2.8
2.6
2.4
2.2
2.0
1.8
1.6
1.4
1.2
1.0
0.8
0.6
0.4
0.2
39
40
41
42
43
44
45
46
47
48
49
50
51
52

FIG.2

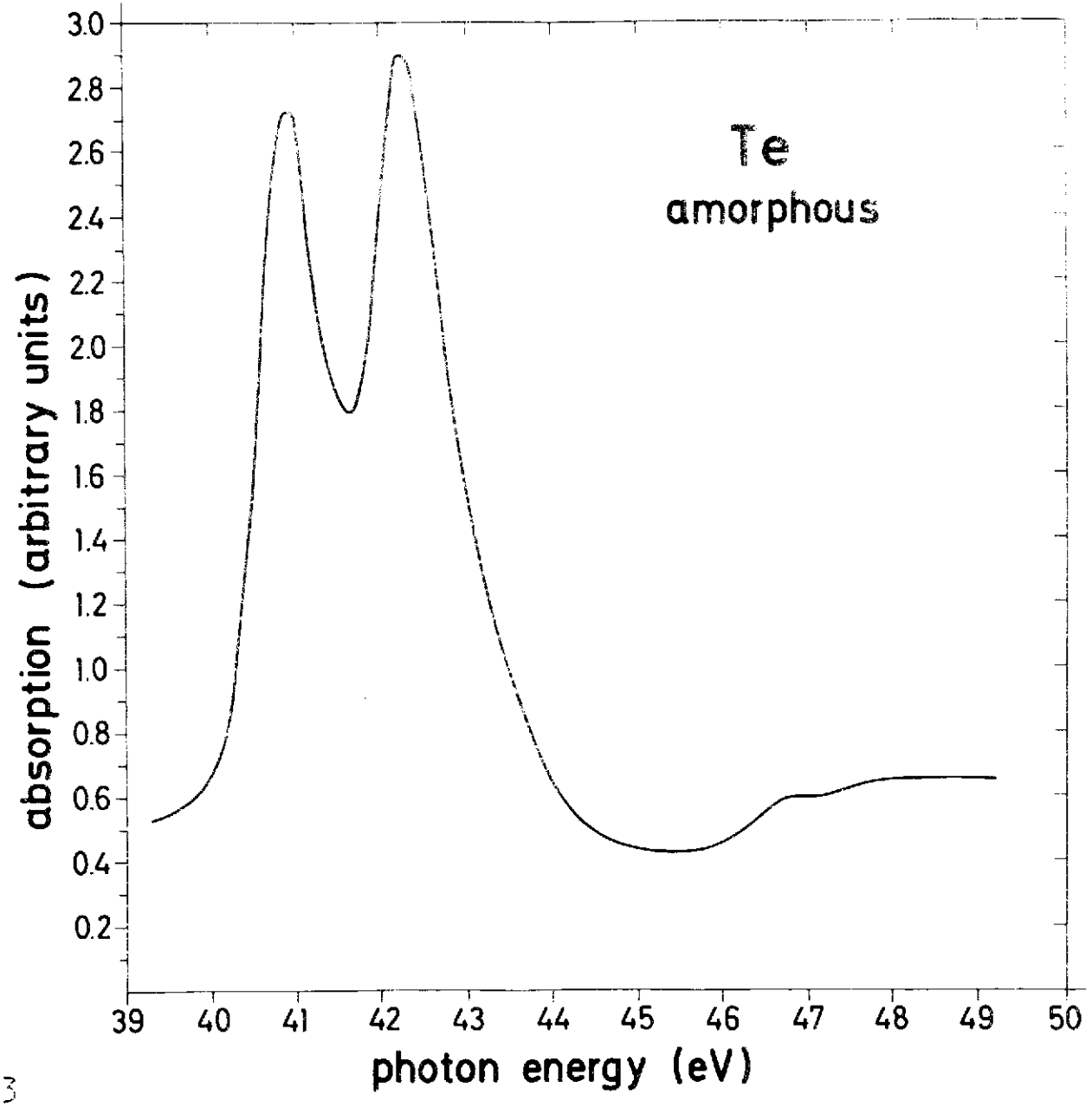
Te
amorphous
absorption (arbitrary units)
photon energy (eV)
3.0
2.8
2.6
2.4
2.2
2.0
1.8
1.6
1.4
1.2
1.0
0.8
0.6
0.4
0.2
39
40
41
42
43
44
45
46
47
48
49
50

FIG.3

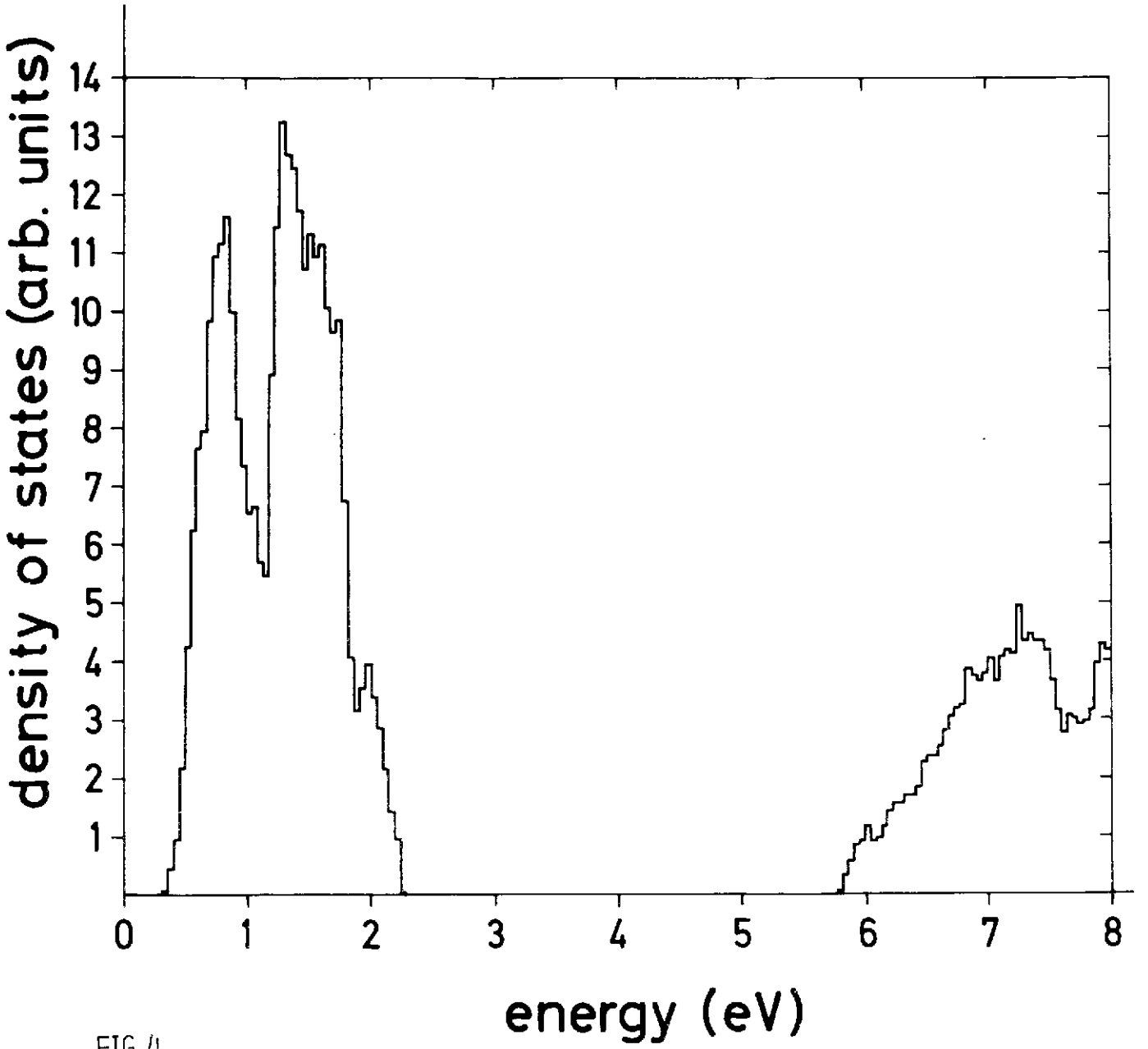
density of states (arb. units)
14
13
12
11
10
9
8
7
6
5
4
3
2
1
0
1
2
3
4
5
6
7
8
energy (eV)

FIG.4